

DoE Award Number: DE-FE0003892

**Multiscale Modeling of Grain Boundary (GB) Segregation
and Embrittlement in Tungsten
for Mechanistic Design of Alloys for Coal Fired Plants**

Jian Luo (PI) & Naixie Zhou

School of Materials Science and Engineering, Clemson University

Vikas Tomar (co-PI), Hong Suk Lee & Niranjan Parab

School of Aeronautics and Astronautics, Purdue University

Program Manager: Dr. Richard Dunst

Outline

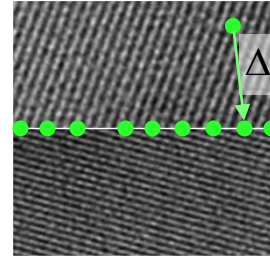
- **Background (Luo)**
- **Thermodynamic Theories & Models (Luo)**
- **Atomistic & Continuum Modeling (Tomar)**

Background:

Grain Boundary (GB) Segregation: Classical & Beyond

McLean-Langmuir Adsorption Model:

$$\frac{\Gamma}{\Gamma_0 - \Gamma} = \frac{X_C}{1 - X_C} \cdot e^{\frac{-\Delta g_{ads}}{kT}}$$



Monolayer?
In reality, not necessarily

Various modifications/extensions exist...

A Bigger Picture?

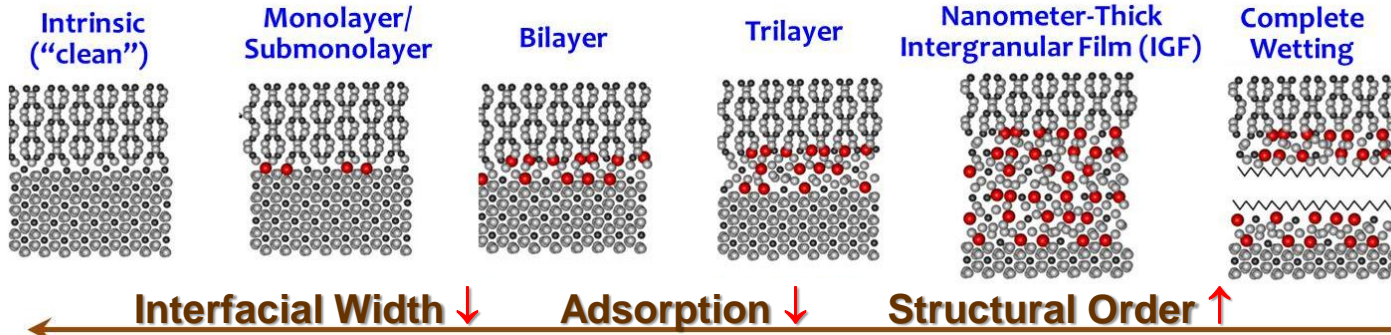


Figure adapted from:
Luo, Cheng, Asl, Kiely & Harmer Science 2011

Also called “complexion”

Earlier publications:
Dillon, Tang, Carter & Harmer Acta Mater. 2007

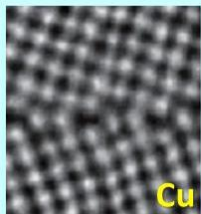
Harmer J. Am. Ceram. Soc. 2010

Classical Langmuir-McLean

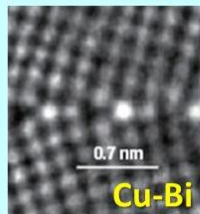
Discrete Thickness ...

Nano “Equilibrium” Thickness

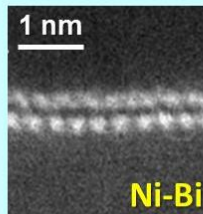
Arbitrarily “Thick” Film



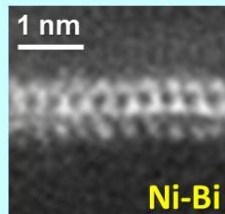
Duscher et al., Nat. Mater. 2004



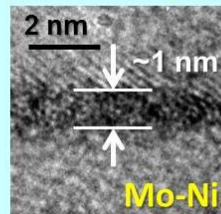
Cu-Bi



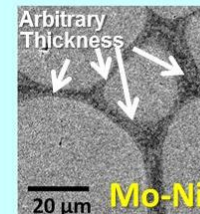
Ni-Bi



Ni-Bi



Mo-Ni



Mo-Ni

Luo et al., Science 2011

Shi & Luo, APL 2009

Broad Background vs. The Focus of This Project:

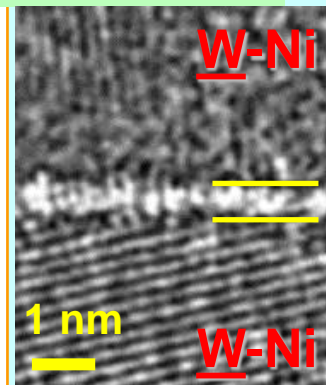
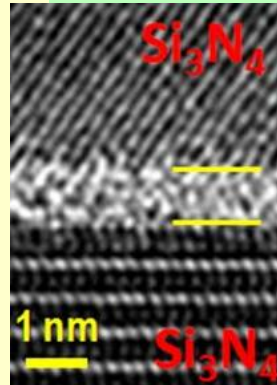
Premelting-Like Segregation in W → Embrittlement

Multilayer Adsorbates!

Equilibrium-Thickness
Intergranular Films (IGFs)

Ubiquitous...

More complex interfacial
interactions (vdW,
electrostatic, etc.)



Subsolidus Quasi-Liquid IGFs

Observed in W, Mo...

Segregation-induced GB
premelting → A new type of GB
segregation occurring at high T
& doping levels?

Background: Broad Technological Implications

Sintering (Classical Theory: Liquid-phase sintering, Kingery *et al.*)

50 Yr Mystery: “Solid-state” activated sintering?

Grain Growth (Classical Theory: Solute-drag, Cahn)

Mystery: Fast “dirty” GBs in Al-Ga, Al_2O_3 ?

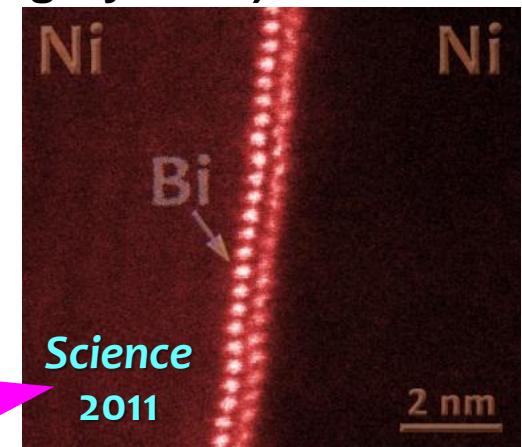
50 Yr Mystery: Abnormal grain growth?

“Unpredictable” Properties?

- Mechanical properties of Si_3N_4 , SiC *etc.*
- Embrittlement of metals

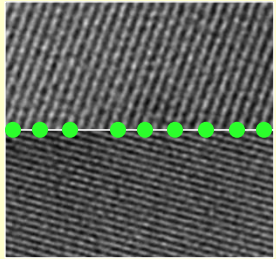
100-Yr Mystery: Liquid metal embrittlement? →

- **Beneficial or Detrimental Physical Properties:** ZnO-Bi₂O₃ (nonlinear I-V); LiFePO₄ (ionic conductivities & charge rates); YBCO superconductor (I_{critical}); RuO₂-based resistors (σ); AlN substrate (κ), ...



Re-appraisal of GB Embrittlement Mechanisms for high- T 's and/or high dopant/impurity activities?

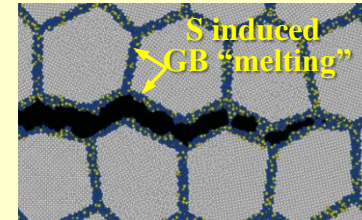
Classical GB Embrittlement Models Built on Langmuir-McLean Adsorption



- Reduction of cohesion due to:
- Electronic effect (weakening the bonds);
 - Atomic size (strain) effect; or
 - Changing relative γ 's (the Rice-Wang Model)

Beyond Monolayer?

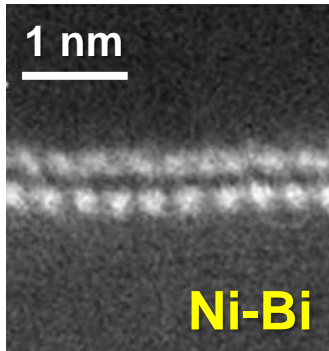
Ni-S (Indirect Evidence)



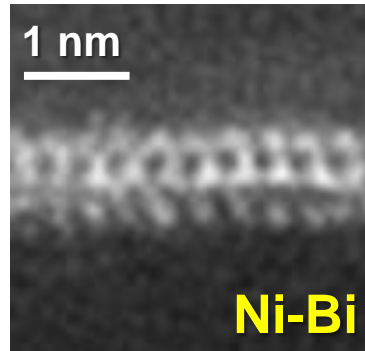
- S segregation
→ GB "melting" if $C_S^{GB} > 15\%$
→ GB Embrittlement

Atomistic Simulation: Chen *et al.*, PRL 2010
FrAuger: Heuer *et al.*, J. Nuclear Mater. 2002

Discrete Thickness



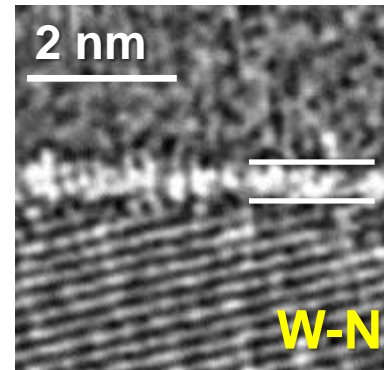
Ni-Bi



Ni-Bi

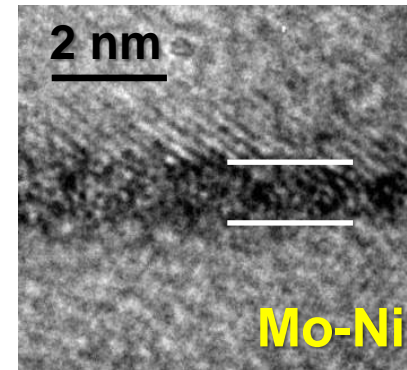
Luo, Cheng, Asl, Kiely & Harmer
Science 333:1730 (2011)

Nanometer "Equilibrium" Thickness



W-Ni

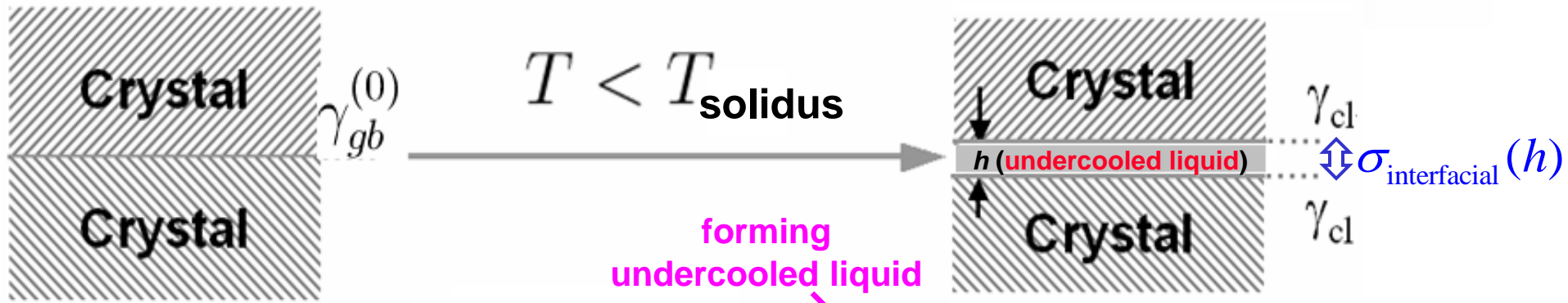
Acta Mater. 55, 3131 (2007)



Mo-Ni

APL 94, 251908 (2009)

Thermodynamic Principle and Model



A subsolidus quasi-liquid film is thermodynamically stable if:

$$\Delta G_{amorph} \cdot h < -\Delta\gamma \equiv \gamma_{gb}^{(0)} - 2\gamma_{cl}$$

The Excess Free Energy:

$$G^x - \gamma_{gb}^{(0)} = \Delta G_{amorph} \cdot h + \Delta\gamma + \sigma_{interfacial}(h) = \Delta G_{amorph} \cdot h + \Delta\gamma \cdot f(h)$$

Interfacial (Disjoining) Potential

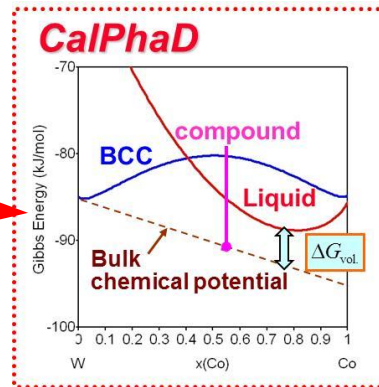
Interfacial Coefficient

$$\begin{cases} f(0) \equiv 0 \\ f(\infty) \equiv 1 \end{cases}$$

Define & quantify:

$$\lambda \equiv \frac{-\Delta\gamma}{\Delta G_{amorph}}$$

Statistical Thermodynamic Model



Continuum approx. for metals:

$$f(h) \approx 1 - e^{-h/\xi}$$

Coherent length

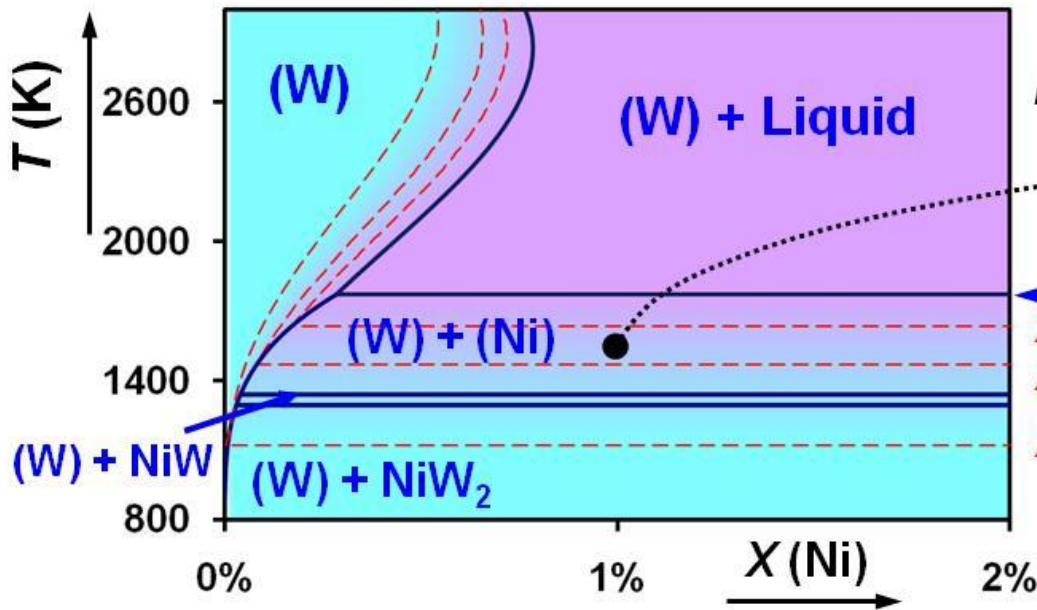
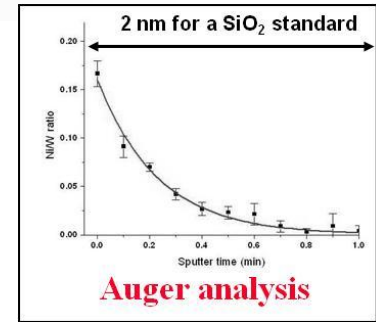
$$h_{EQ} \approx \xi \cdot \ln(\lambda / \xi)$$

Computed Lines of Constant λ : GB Diagrams

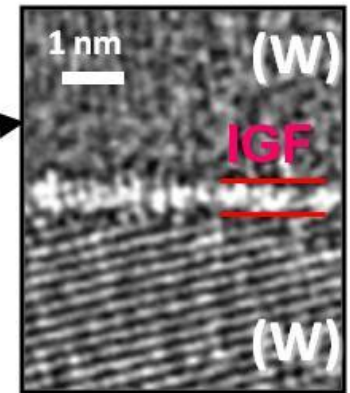
Luo & Shi, *Appl. Phys. Lett.* 2008

W-Ni (an Example)

Gupta, Yoon,
Meyer & Luo
Acta Mater. 2007



Verified by HRTEM:
 $h_{EQ} = \xi \cdot \ln(\lambda / \xi) \approx 0.6 \text{ nm}$



$\lambda = 2 \text{ nm}$ Bulk Solidus
 $\lambda = 1 \text{ nm}$
 $\lambda = 0.5 \text{ nm}$ Approx. GB Solidus

Verified by onset sintering $T = 1150 \pm 18 \text{ K}$
(~1 monolayer of quasi-liquid film)

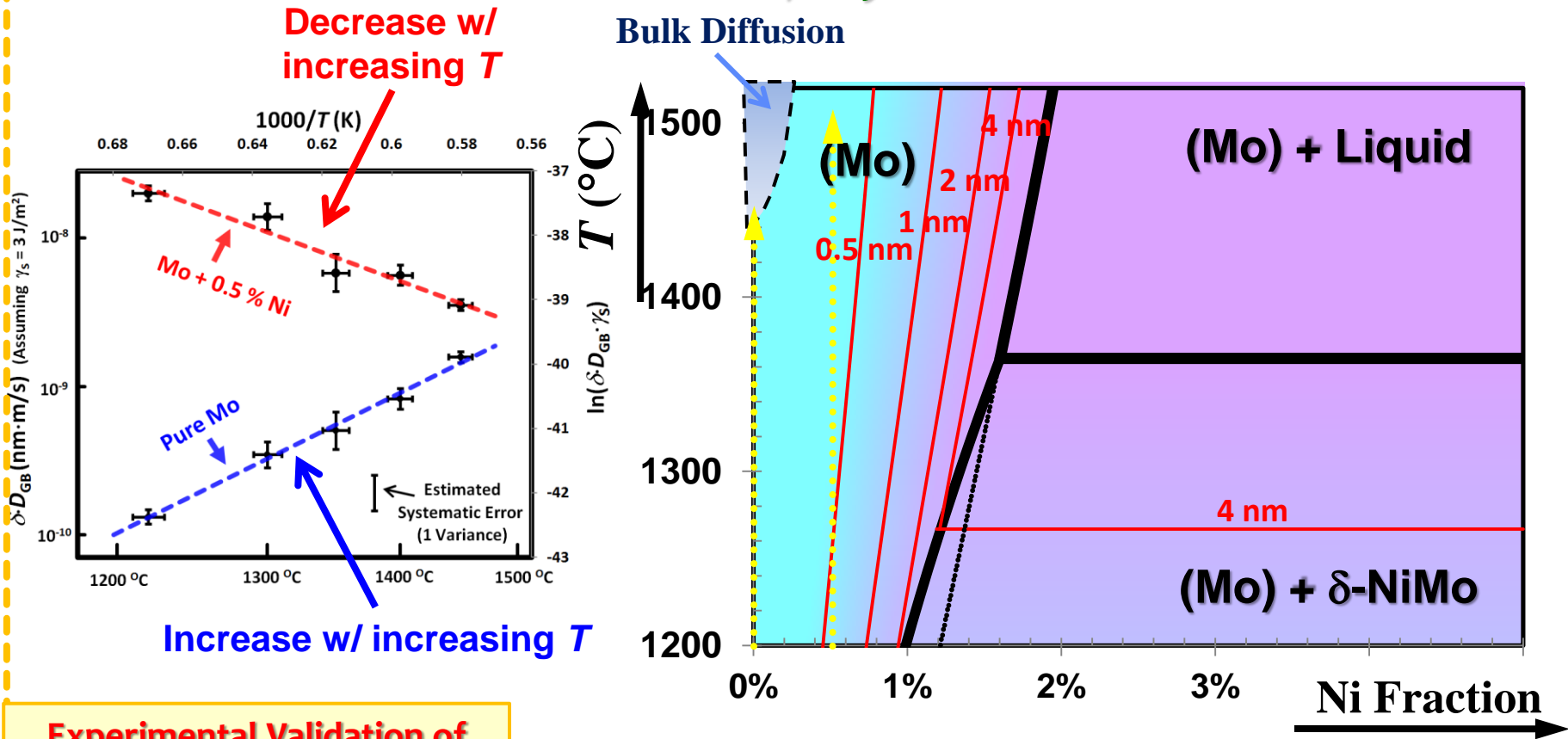
$$h_{EQ} \approx \xi \cdot \ln(\lambda / \xi)$$

One of the goals of this project: Combining multiscale modeling (@ Purdue) to forecast embrittlement

Predictability & Usefulness Demonstrated!

E.g., Retrograde Solubility \rightarrow Decreasing GB Diffusivity w. Increasing T ?

Shi & Luo, *Phys. Rev. Lett.* 2010



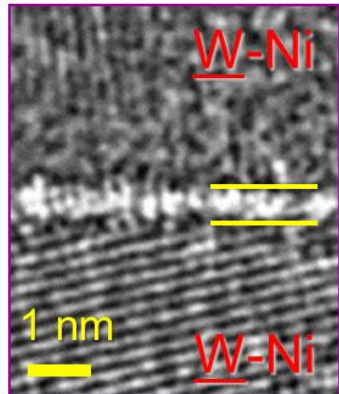
Objectives of This UCR Project

Using **W based binary & ternary alloys** as model systems...

- I. Development of thermodynamic theories and models to compute “GB diagrams” (binary \rightarrow multicomponent)
- II. Quantum, atomistic and continuum modeling to link GB segregation with GB embrittlement (Purdue/Tomar)
- III. Validation

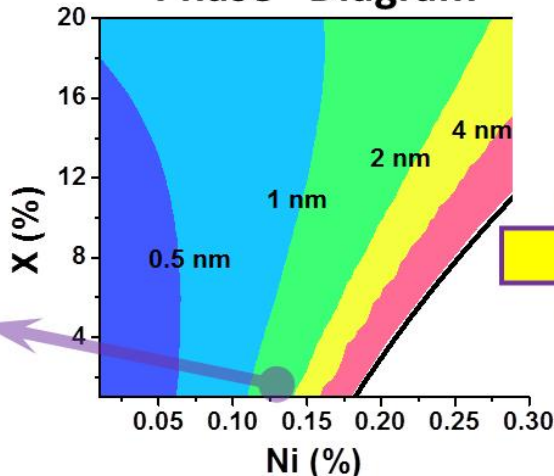
Overview

HR-TEM

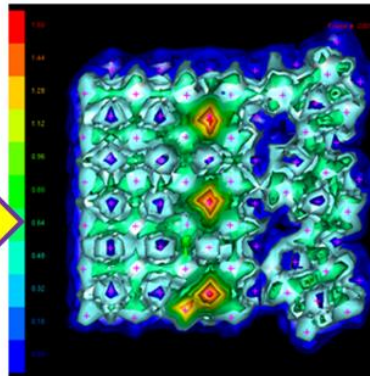


Clemson (Luo *et al.*)

Computed Grain Boundary
“Phase” Diagram

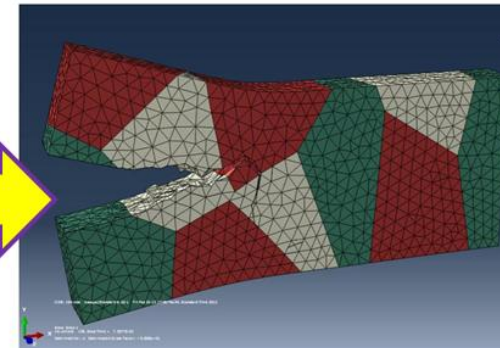


Car-Parrinello
Molecular Dynamics



Purdue (Tomar *et al.*)

3D Extended
Finite Element Method



One of the Major Goals of This UCR Project

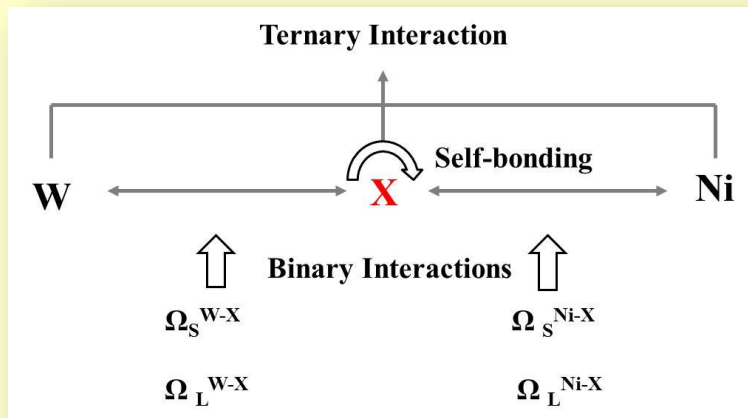
Extend Models from Binary to Multicomponent Systems (Using W Alloys as Model Systems)

Rationale: Practical Important!

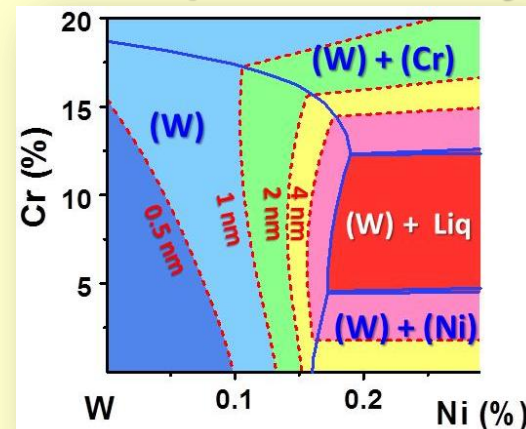
- Engineering alloys often have multiple alloying elements or impurities
- Offering a way to use co-alloying to control GB behaviors

Mathematical Formulation
(Development & validation of
the theory and model)

Numerical Experiments



Examples of Real Systems

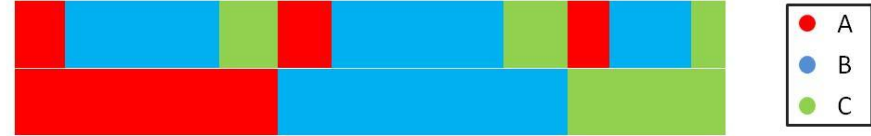


W-Cr-Ni
1400 °C

Mathematical Formulation for Multicomponent Alloys

$$\lambda \equiv \frac{\gamma_{GB}^{(0)} - 2\gamma_{cl}}{\Delta G_{amorph}}$$

$$\gamma_{GB}^{(0)} = \sum_i^n \frac{F_i^S \Delta H_i^{\text{vaporization}}}{3C_0 V_i^{2/3}} \gamma$$



Miedema type model (Yr. 1)

$$\gamma_{cl} = \sum_i^n \frac{F_i^S \Delta H_i^{\text{fuse}}}{C_0 V_i^{2/3}} + \sum_{j \neq i} \sum_i^n \frac{F_i^S F_i^L \Delta H_{j \text{ in } i}^{\text{interface}}}{C_0 V_j^{2/3}} + \frac{1.9RT}{C_0 V_{\text{average}}^{2/3}} - \gamma_{cl}^{(\text{Ref.})}$$



$$V_{i-j}^{2/3} = 2V_i^{2/3}V_j^{2/3} / (V_i^{2/3} + V_j^{2/3}), \quad 4\omega_{i-j}^L = F_i^L \Delta H_{j \text{ in } i}^{\text{interface}} + F_j^L \Delta H_{i \text{ in } j}^{\text{interface}} \Big|_{X_i=X_j=0.5}$$

Modified; using regular-solution parameters (New for Yr. 2!)

$$\gamma_{cl} = \sum_i^n \frac{F_i^S \Delta H_i^{\text{fuse}}}{C_0 V_i^{2/3}} + \sum_{j \neq i} \sum_i^n \frac{F_i^S F_i^L \omega_{i-j}^L}{C_0 V_{i-j}^{2/3}} + \frac{1.9RT}{C_0 V_{\text{average}}^{2/3}} - \gamma_{cl}^{(\text{Ref.})}$$

Can be obtained from CalPhaD

ΔG_{amorph} by CalPhaD

$$\Delta G_{amorph} = G^{\text{liquid}}(\mathbf{X}_{\text{film}}) - \sum_i^n \mu_i^{\text{solid}} X_i^{\text{film}}$$

More consistence; Applicable beyond transition metals

For each phase ϕ :

$$G^\phi = \sum_i X_i \cdot {}^0 G_i^\phi + RT \sum_i X_i \ln X_i + {}^{XS} G^\phi$$

Redlich-Kister-Muggianu:

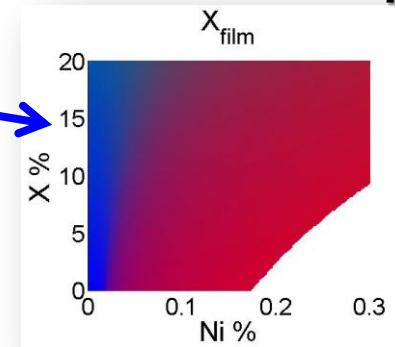
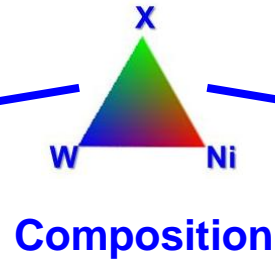
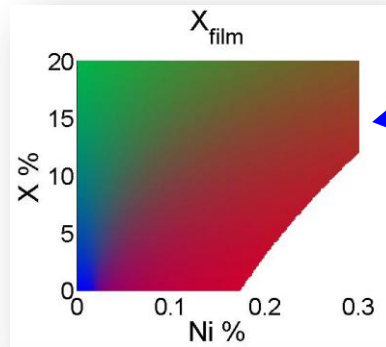
$${}^{XS} G^\phi = \sum_{i \neq j}^n L_m^\phi X_i X_j (X_i - X_j)^m + \text{high - order term(s)}$$

Numerical Experiment (I)

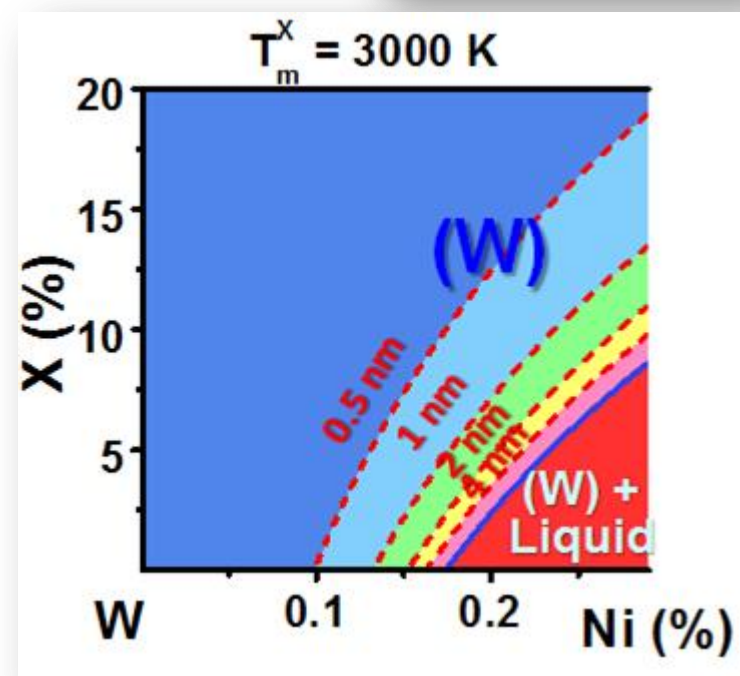
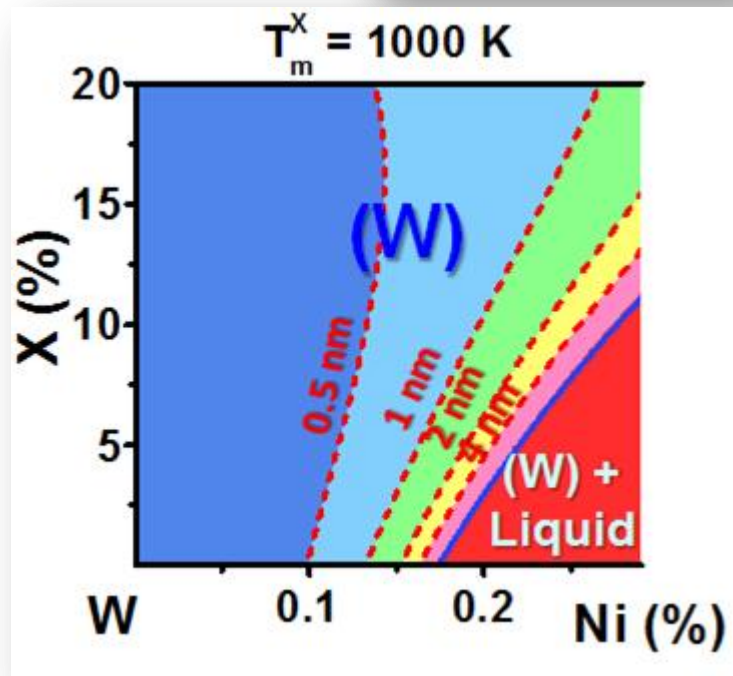
W-Ni-X Ternary Alloy

W-X & W-Ni are ideal solutions for both liquid and solid (BCC) phases;
 $\Delta S^{\text{fuse}} \sim 10 \text{ J/mol}\cdot\text{K}$; $\Delta H_X^{\text{fuse}} / \Delta H_X^{\text{vap}} = 0.04$

$T = 1673 \text{ K}$



GB λ -diagrams



T_{melt} of co-dopant (X) does not affect significantly!

Numerical Experiment (II)

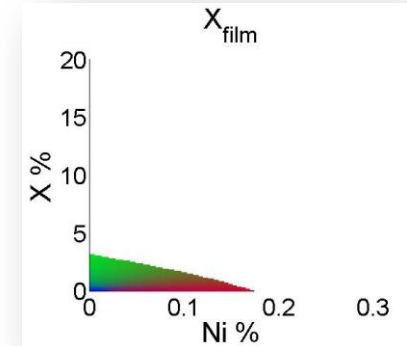
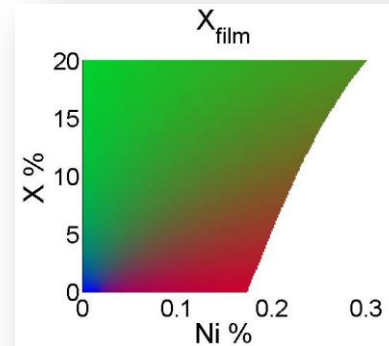
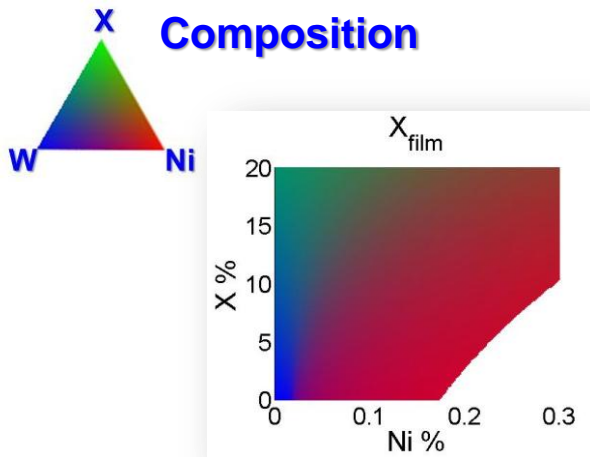
W-Ni-X Ternary Alloy

W-X L, Ni-X S/L are ideal solutions;

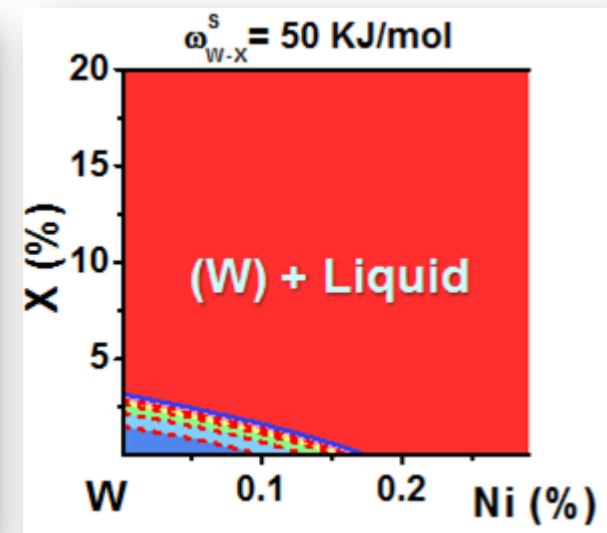
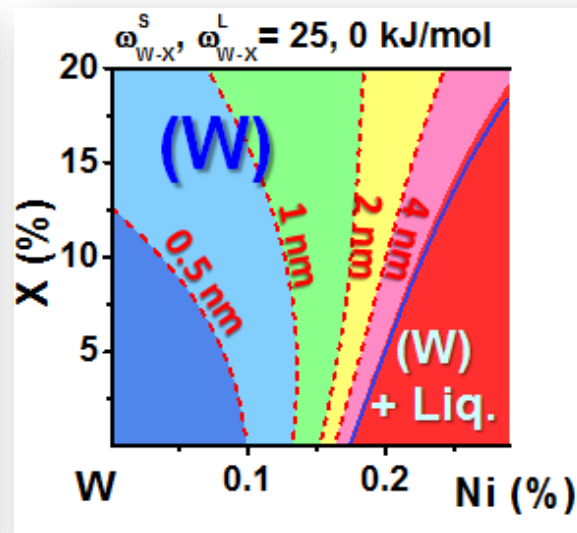
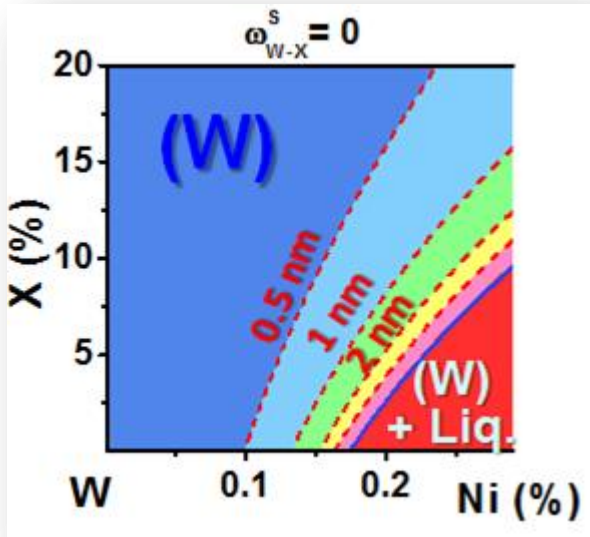
$$T_M^X = 1750\text{K}$$

Solid $\omega_{W-X}^S \rightarrow$ representing ΔH_{seg} .

$$T = 1673\text{K}$$



GB λ -diagrams



Increasing Segregation Tendency of X (represented by ω_{W-X}^S)...

Numerical Experiment (III)

W-Ni-X Ternary Alloy

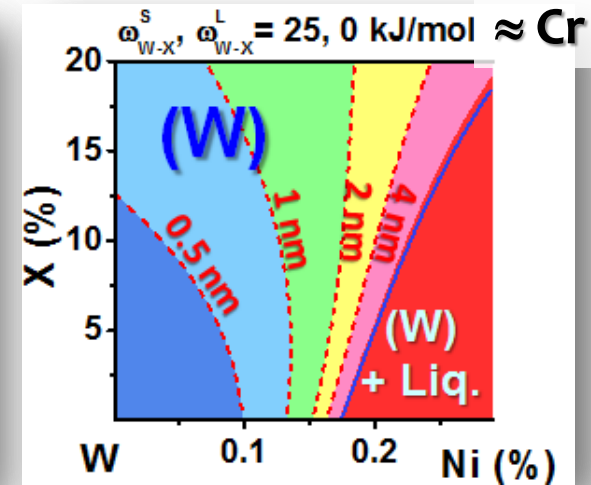
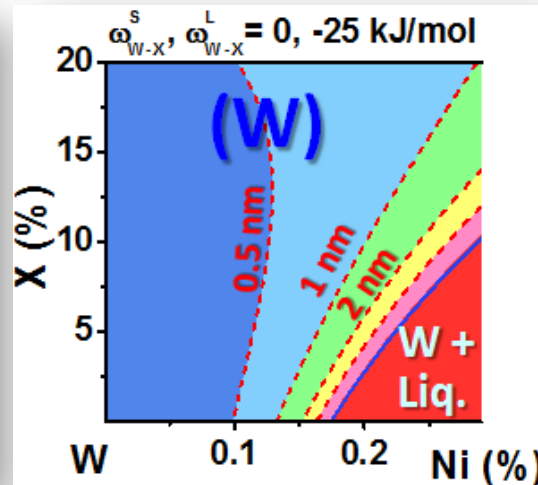
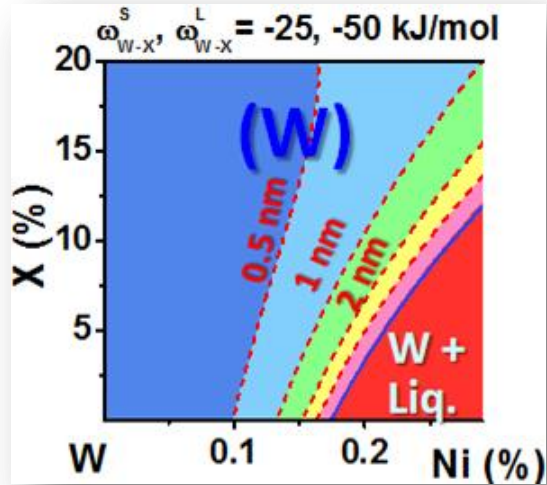
Ni-X S/L are ideal solutions; $T_M^X = 1750\text{K}$
 Varying ω_{W-X}^S & ω_{W-X}^L $T = 1673\text{K}$

$$\omega_{W-X}^L = -50 \text{ kJ/mol}$$

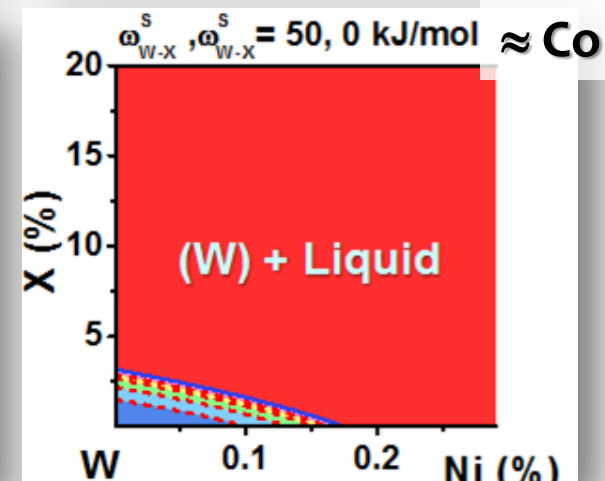
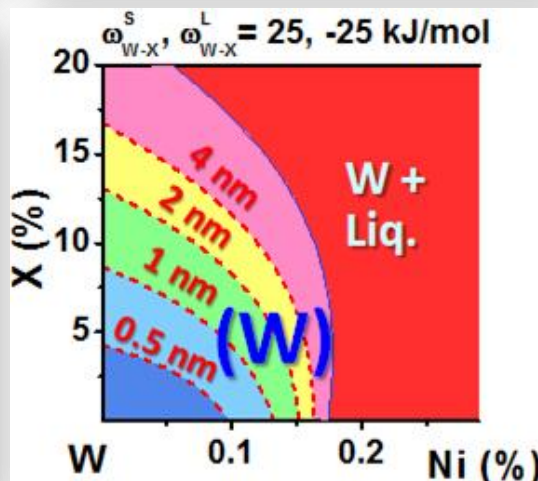
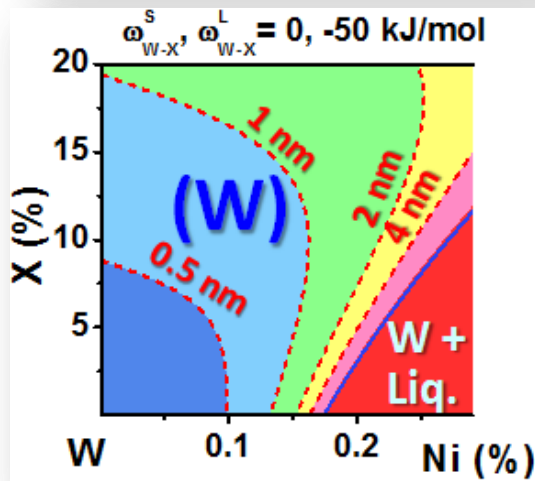
$$\omega_{W-X}^L = -25 \text{ kJ/mol}$$

$$\omega_{W-X}^L = 0 \text{ kJ/mol} \approx \text{Cr}$$

$$\omega_{W-X}^S - \omega_{W-X}^L = +25 \text{ kJ/mol}$$



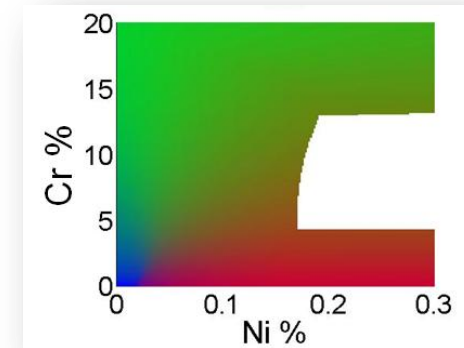
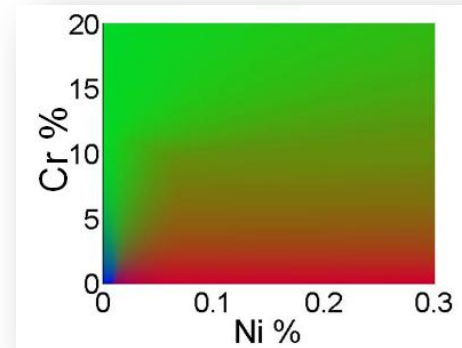
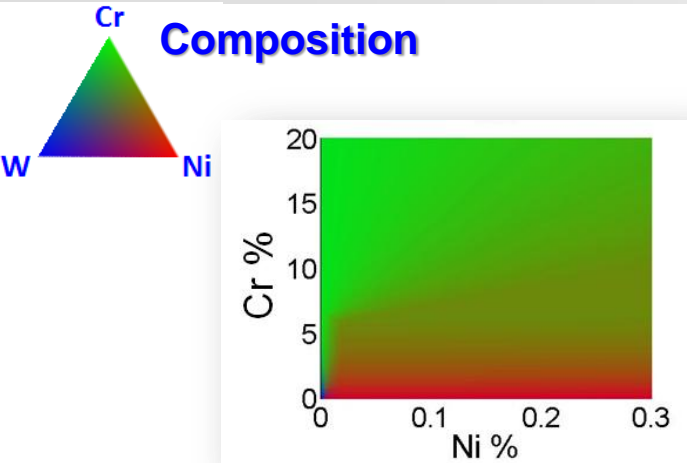
$$\omega_{W-X}^S - \omega_{W-X}^L = +50 \text{ kJ/mol}$$



More negative ω_{W-X}^L (tendency for mixing in liquid \uparrow)...

Example of a Real System: W-Ni-Cr Ternary Alloy

W-Ni-Cr bulk CalPhaD data from: Gustafson, CALPHAD 12, 277 (1988)

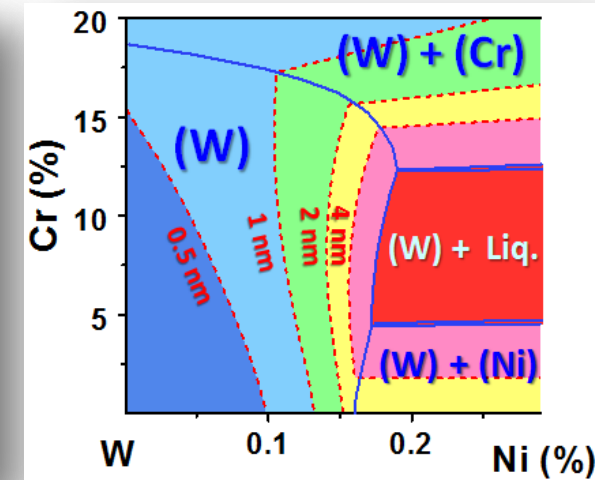
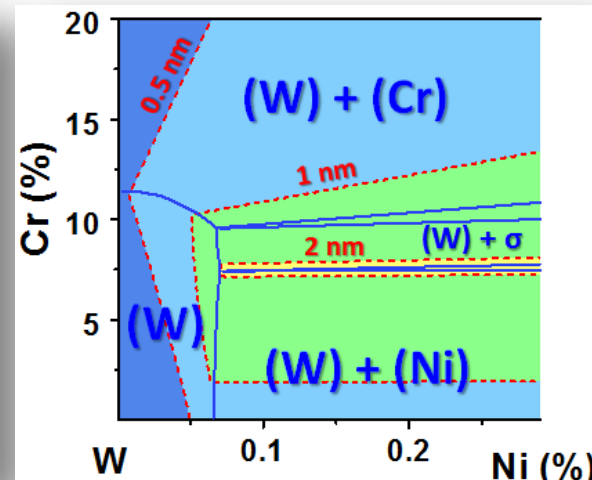
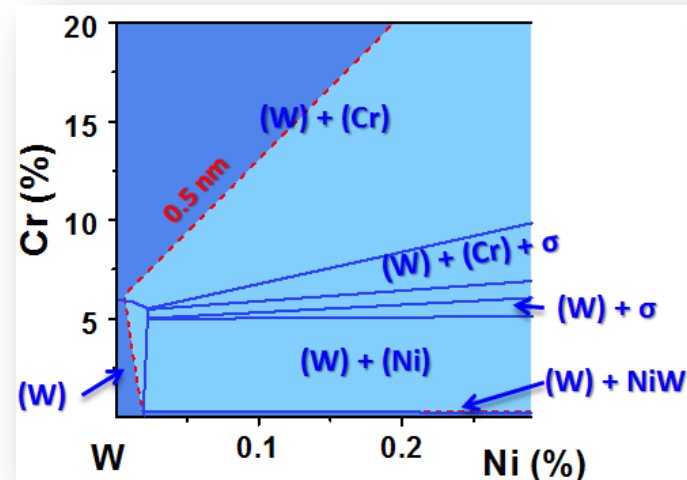


GB λ -diagrams

$T = 1000 \text{ }^\circ\text{C}$

$T = 1200 \text{ }^\circ\text{C}$

$T = 1400 \text{ }^\circ\text{C}$

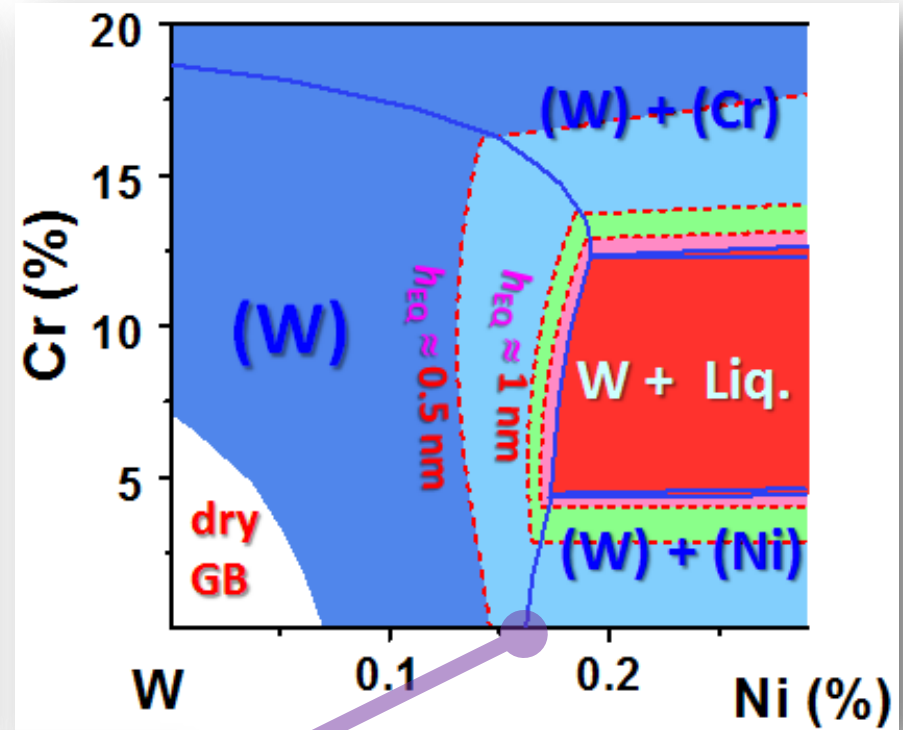
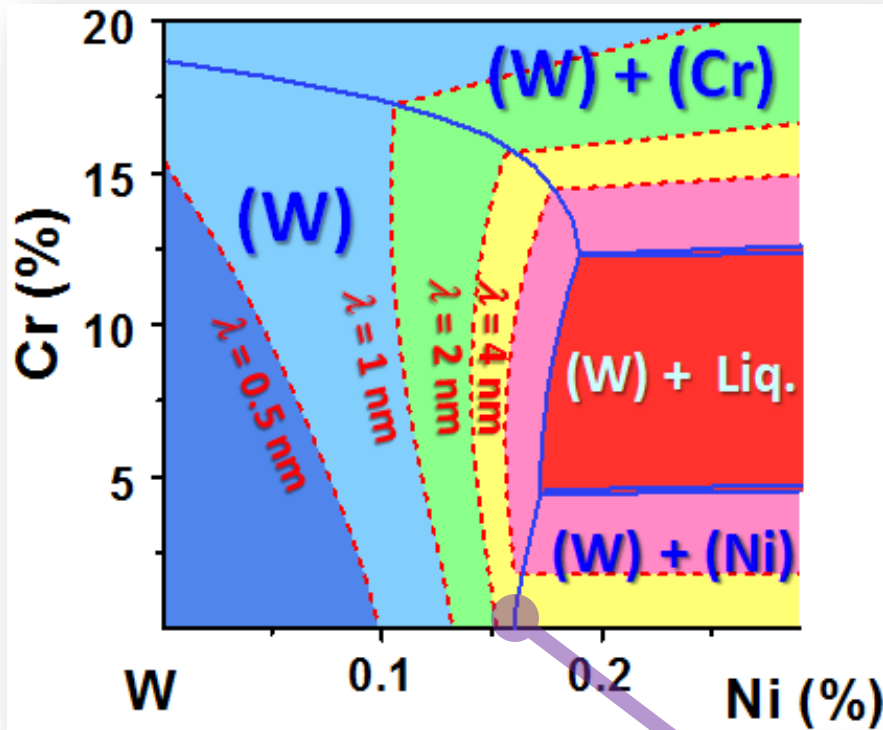


Increasing Temperature...

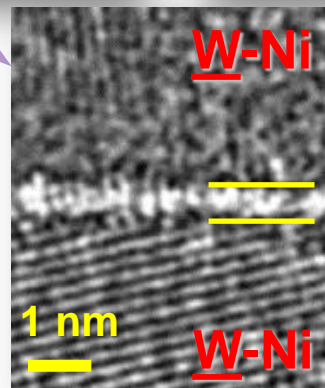
W-Ni-Cr (1400 °C): from λ to h_{EQ} (interfacial width)?

GB λ -diagram

Estimated h_{EQ}



Ni-Saturated W
(1400 °C)



$$h_{EQ} \approx \xi \cdot \ln(\lambda / \xi)$$

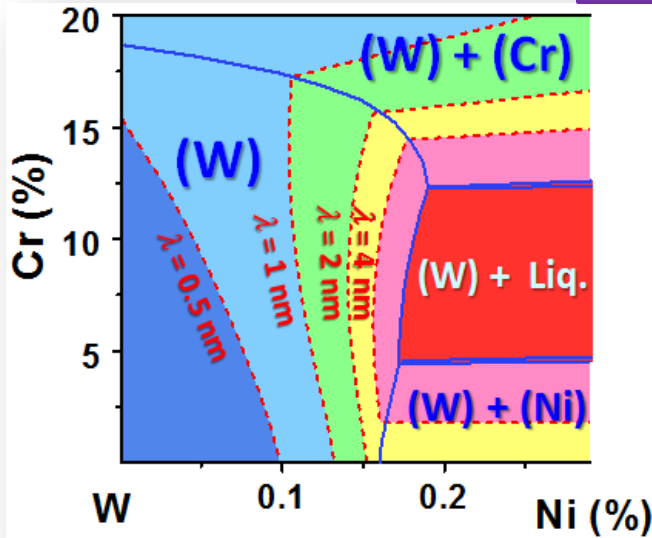
$$\lambda = 2.1 \text{ nm} \Leftrightarrow h_{EQ} = 0.6 \text{ nm}$$

$$\Rightarrow \xi \approx 0.318 \text{ nm}$$

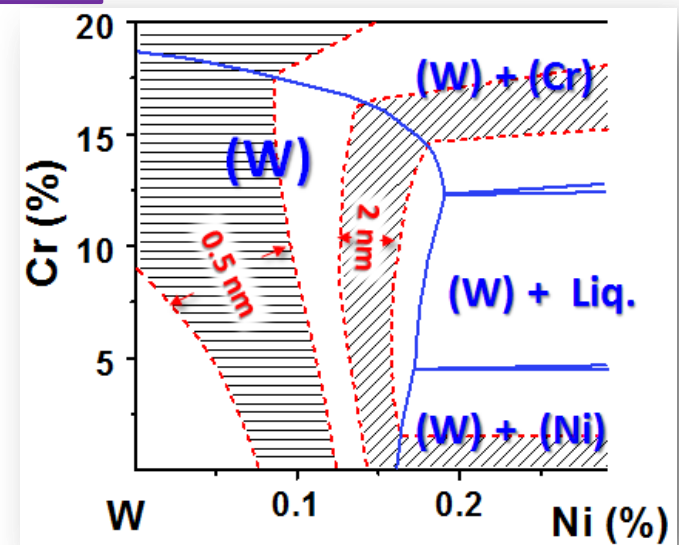
W-Ni-Cr (1400 °C): GB-to-GB Variation

Average GBs:

Computed GB λ -diagram

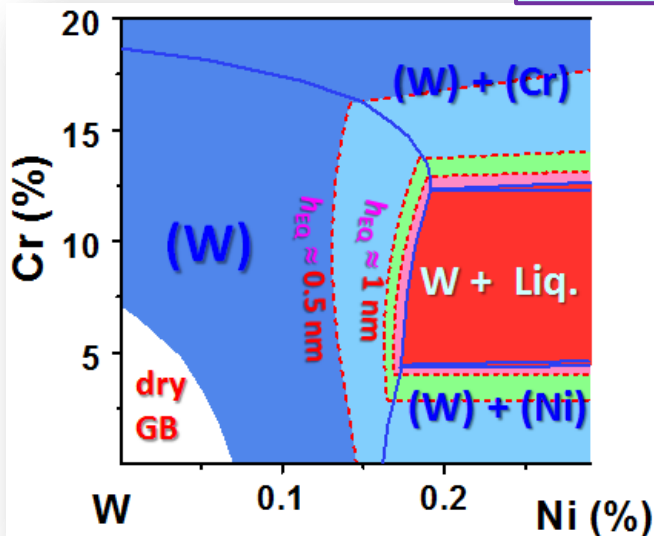


Assuming $\gamma_{GB}^{(o)}$ varies by $\pm 15\%$

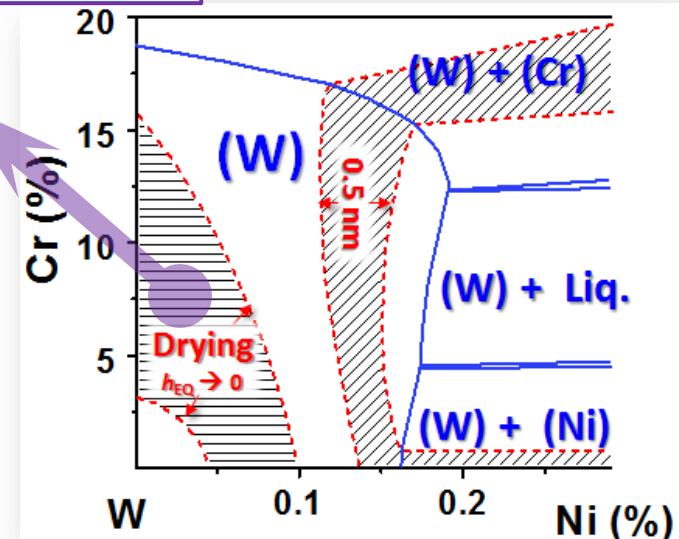


Average GBs:

Estimated Interfacial Width (h_{EQ})



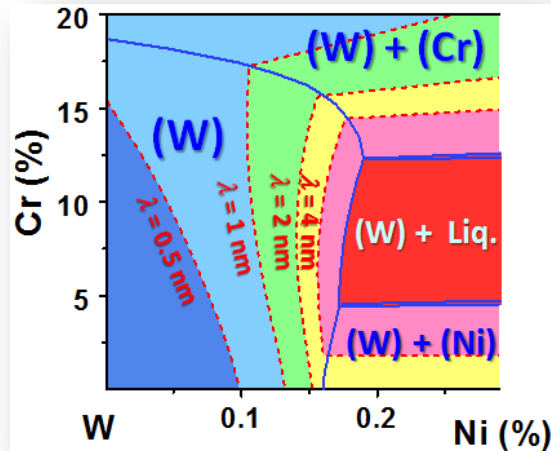
Assuming $\gamma_{GB}^{(o)}$ varies by $\pm 15\%$



A Useful Component for the “Materials Genome” Project?

Construct GB “Phase” Diagrams

Prior work : Straumal et al., *Interf. Sci.* 2004; Tang et al., *PRL* 2006;
Dillon, Tang, Carter, Harmer, *Acta Mater.* 2007



GB “phase” diagrams

Design:

- Fabrication protocols utilizing appropriate GB structures to achieve optimal microstructures
- Co-doping strategies and/or heat treatment recipes to tune the GB structures for desired performance

R. M. Cannon *et al.*

For example:

- Utilizing liquid-like GB structures for low T sintering
- A heat treatment to “dry” GBs for remediate embrittlement?

Applications: To predict useful trends in:

- Grain boundary embrittlement
- Sintering
- Grain growth & microstructural involution
- GB controlled creep, corrosion & oxidation
- ...

A useful component for
“Materials Genome”?

Summary & Future Work – Part I

In the “thermodynamics” thrust, we have ...

- Derived the basic equations to extend our models from binary to multicomponent alloys;
- Developed and tested the algorithms and MATLAB codes for computing ternary “GB diagrams” numerically; and
- Completed “numerical experiments” and computations for W-Ni-Cr

Milestone 1 achieved by 9/30/2011 (on time):

“Develop a thermodynamic description for high- T premelting-like GB segregation in multicomponent refractory alloys.”

Further Work:

- More “numerical experiments” and computations
- Combine with Purdue’s multiscale modeling → embrittlement
- Validation and further refinements

CAR-PARRINELLO MOLECULAR DYNAMICS

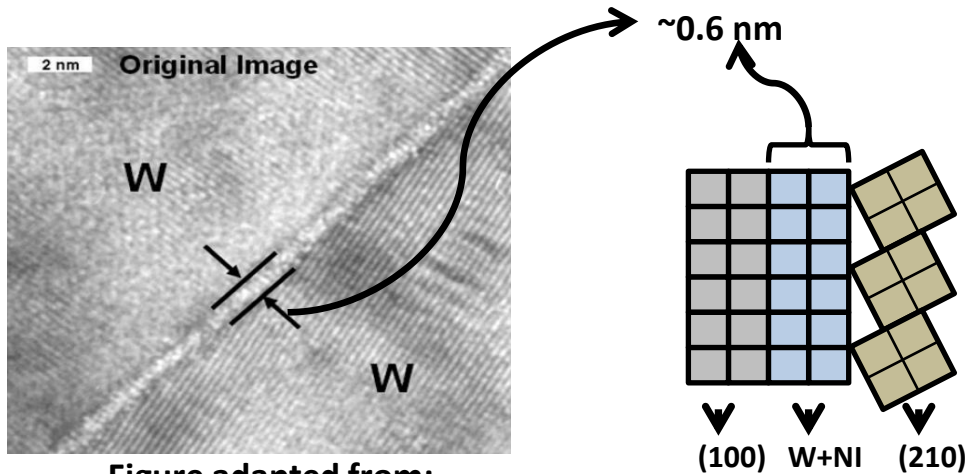
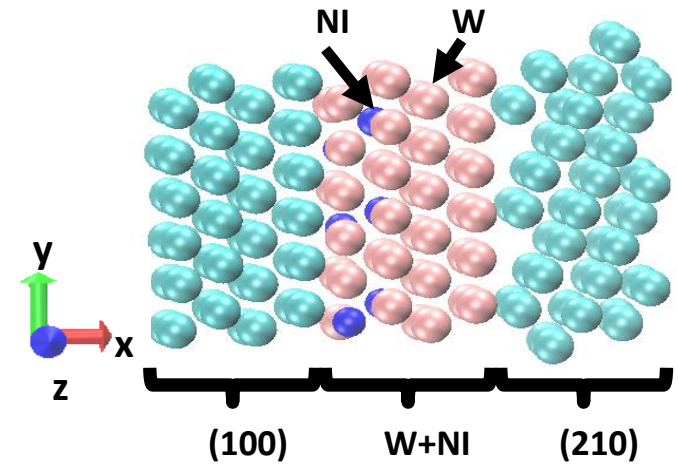
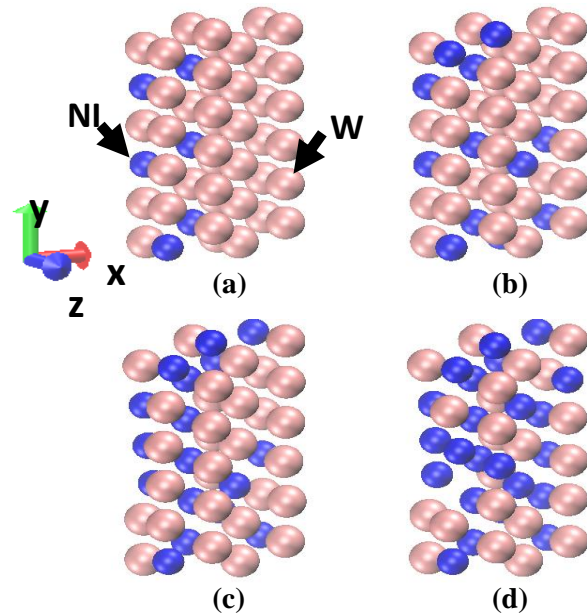


Figure adapted from:
Gupta, Yoon, Meyer, & Luo
Acta Materialia, 2007



Atomic model :
Nickel-doped Tungsten interface



To investigate the effect of Nickel content in the GB region, four different Nickel percentages are embedded while modeling the atomic structures.

- | | | |
|-----|-------------------------------------|----------------|
| (1) | 6 Nickel atoms + 42 Tungsten atoms | → 12.5 at.% Ni |
| (2) | 12 Nickel atoms + 36 Tungsten atoms | → 25 at.% Ni |
| (3) | 18 Nickel atoms + 30 Tungsten atoms | → 37.5 at.% Ni |
| (4) | 24 Nickel atoms + 24 Tungsten atoms | → 50.0 at.% Ni |

CAR-PARRINELLO MOLECULAR DYNAMICS

FORMULATION

The basic idea of the CPMD approach can be viewed to exploit the quantum-mechanical adiabatic time-scale separation of fast electronic and slow nuclear motion by transforming that into classical-mechanical adiabatic energy-scale separation in the framework of dynamical systems theory.

Car and Parrinello postulated the following class of Lagrangians

$$L_{CP} = \underbrace{\sum_I \frac{1}{2} M_I \dot{R}_I^2 + \sum_i \frac{1}{2} \mu_i \langle \dot{\psi}_i | \dot{\psi}_i \rangle}_{\text{Kinetic energy}} - \underbrace{\langle \Psi_0 | H_e | \Psi_0 \rangle}_{\text{Potential energy}} + \underbrace{\text{constraints}}_{\text{Orthonormality}}$$

The corresponding Newtonian equations of motion are obtained from the associated Euler-Lagrange equations

$$\frac{d}{dt} \frac{\partial L}{\partial \dot{R}_I} = \frac{\partial L}{\partial R_I}$$

$$\frac{d}{dt} \frac{\delta L}{\delta \dot{\psi}_i^*} = \frac{\delta L}{\delta \psi_i^*}$$

Following this route of ideas, generic Car-Parrinello equations of motion are found to be of the form

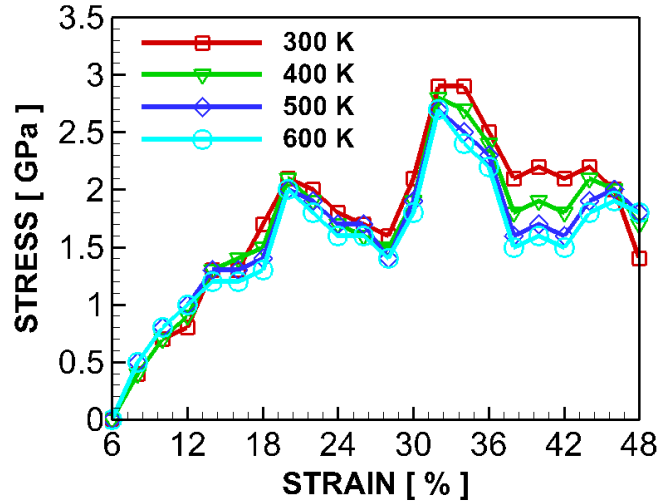
$$M_I \ddot{R}_I(t) = - \frac{\partial}{\partial R_I} \langle \Psi_0 | H_e | \Psi_0 \rangle + \frac{\partial}{\partial R_I} \{\text{constraints}\}$$

$$\mu_i \ddot{\psi}_i(t) = - \frac{\delta}{\delta \psi_i^*} \langle \Psi_0 | H_e | \Psi_0 \rangle + \frac{\delta}{\delta \psi_i^*} \{\text{constraints}\}$$

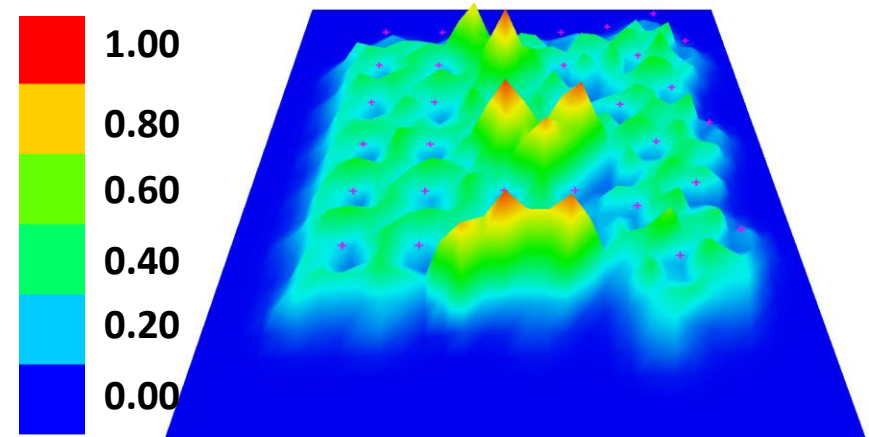
where μ_i ($= \mu$) are the “fictitious masses” or inertia parameters assigned to the orbital degrees of freedom

CAR-PARRINELLO MOLECULAR DYNAMICS

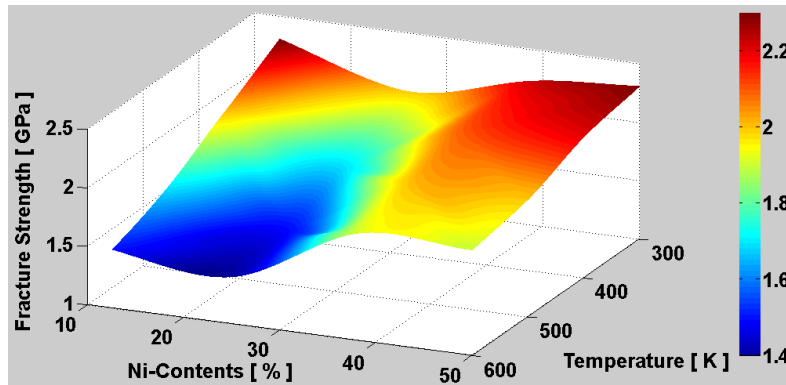
RESULT



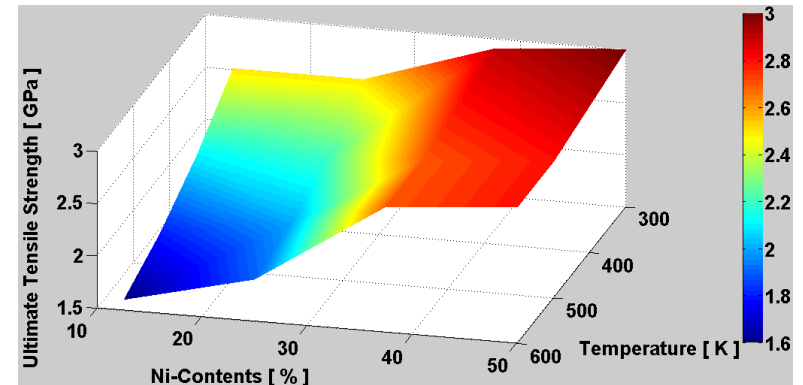
Stress-Strain relation from CPMD calculation



Electron density contour



Fracture strength



Ultimate Tensile Strength

$$f(n,t) = 6.489 - (0.246) \cdot n - (1.016 \times 10^{-2}) \cdot t + (7.047 \times 10^{-3}) \cdot n^2 + (2.53 \times 10^{-4}) \cdot n \cdot t + (5.332 \times 10^{-6}) \cdot t^2 - (6.655 \times 10^{-5}) \cdot n^3 - (1.97 \times 10^{-6}) \cdot n^2 \cdot t - (6.718 \times 10^{-8}) \cdot n \cdot t^2$$

$$f(n,t) = 6.489 - (0.246) \cdot n - (1.016 \times 10^{-2}) \cdot t + (7.047 \times 10^{-3}) \cdot n^2 + (2.53 \times 10^{-4}) \cdot n \cdot t + (5.332 \times 10^{-6}) \cdot t^2 - (6.655 \times 10^{-5}) \cdot n^3 - (1.97 \times 10^{-6}) \cdot n^2 \cdot t - (6.718 \times 10^{-8}) \cdot n \cdot t^2$$

n: percentage of nickel, t: temperature

EXTENDED FINITE ELEMENT METHOD

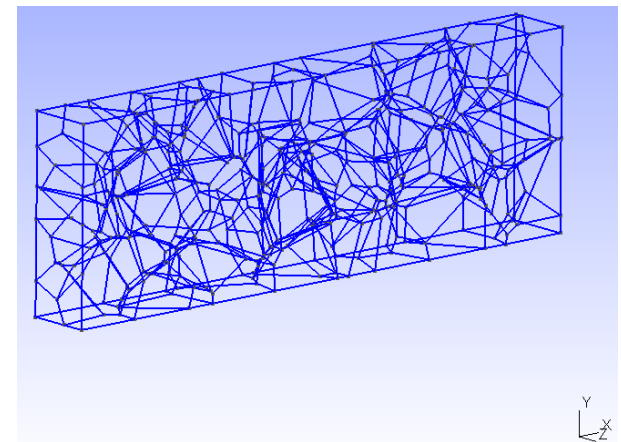
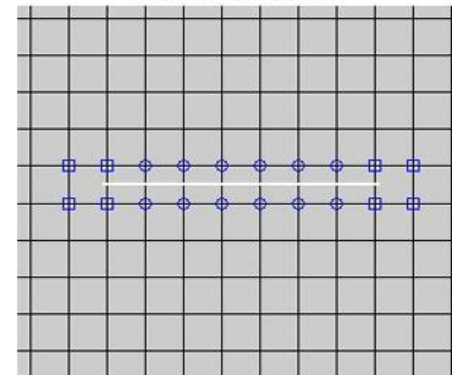
➤ Microscale simulation is now conducted using the parameters obtained from the result of Car-Parrinello Molecular Dynamics.

➤ Extended Finite Element Method(XFEM) is used to predict the crack propagation of three-dimensional polycrystalline material.

➤ XFEM is firstly introduced in 1999 by the work of Black and Belytschko, XFEM is a local partition of unity (PUM) enriched finite element method.

➤ Three-dimensional polycrystalline microstructure is designed using NEPER which makes being able to control the grain growth by Voronoi tessellation.

Enriched Nodes for Crack



EXTENDED FINITE ELEMENT METHOD FORMULATION

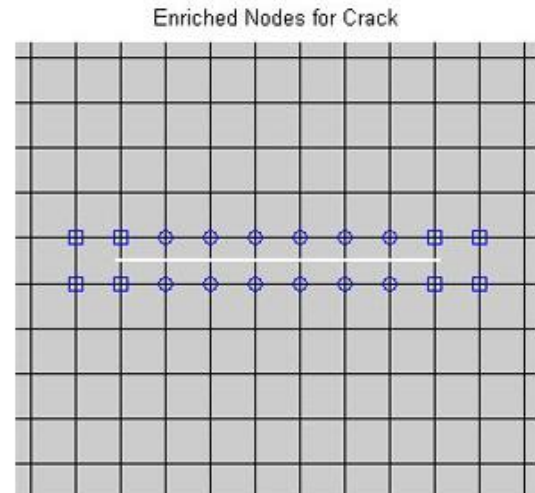
$$u^h(x) = \sum_I N_I(x)u_I + \sum_I N_I(x)v(x)a_I$$

The extended finite element method (XFEM) uses the partition of unity framework to model strong and weak discontinuities independent of the finite element mesh. This allows discontinuous functions to be implemented into a traditional finite element framework through the use of enrichment functions and additional degrees of freedom.

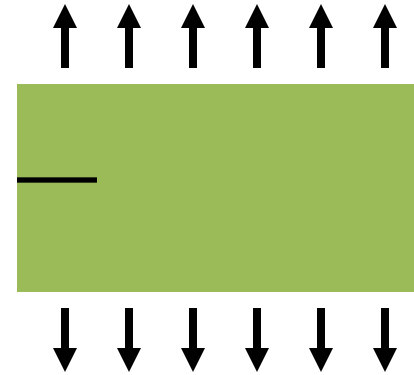
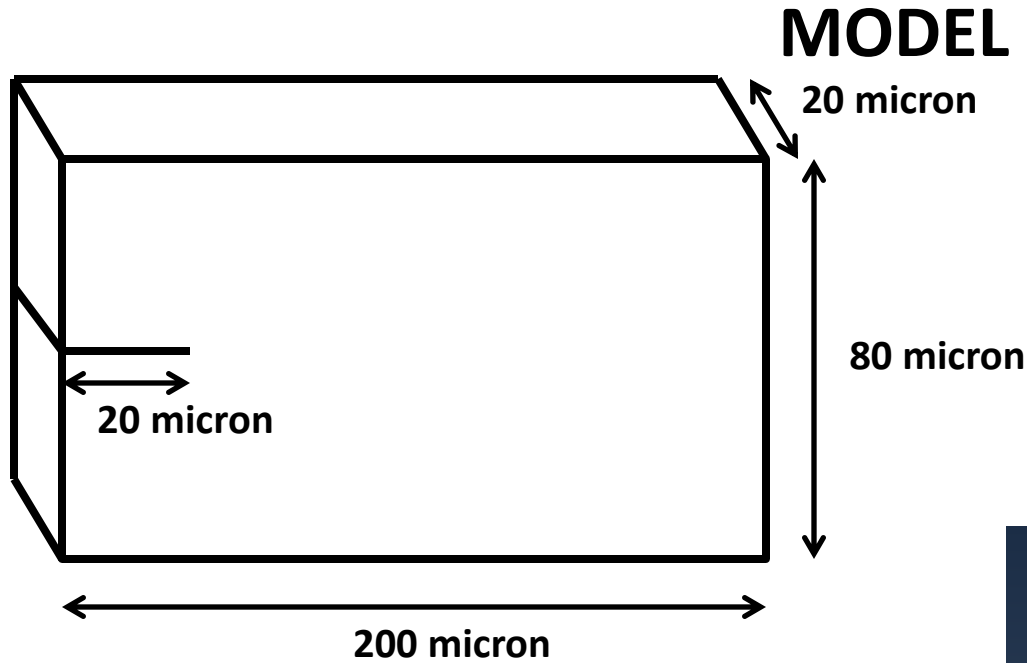
Crack :
$$v_a(x) = \left[\sqrt{r} \sin \frac{\theta}{2}, \sqrt{r} \cos \frac{\theta}{2}, \sqrt{r} \sin \theta \sin \frac{\theta}{2}, \sqrt{r} \sin \theta \cos \frac{\theta}{2} \right]$$





Material Interface :
$$v(x) = \sum_I N_I |\zeta_I| - \left| \sum_I N_I \zeta_I \right|$$

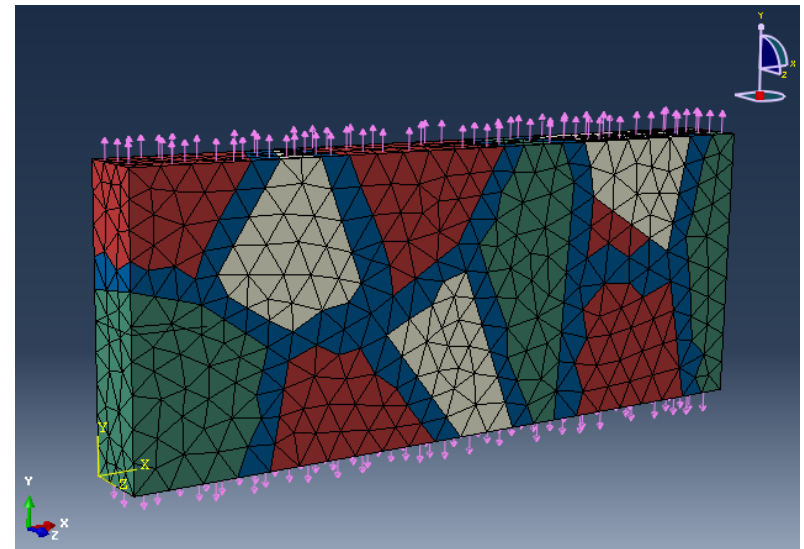
Void :
$$u^h(x) = V(x) \sum_I N_I(x)u_I$$



3-D POLYCRYSTALLINE MICROSTRUCTURE



- Material 1:  $E=300\text{Gpa}$, $\nu=0.28$, $T=250\text{Mpa}$
 - Material 2:  $E=400\text{Gpa}$, $\nu=0.28$, $T=200\text{Mpa}$
 - Material 3:  $E=500\text{Gpa}$, $\nu=0.28$, $T=150\text{Mpa}$
 - Interface :  $E=15\text{Gpa}$, $\nu=0.28$, $T=3000\text{Mpa}$
- Displacement at failure : 0.1 microns

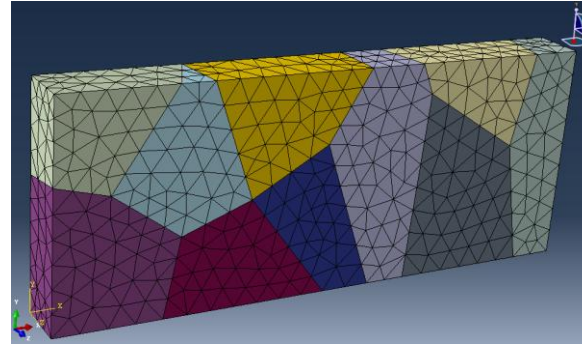


LOAD : SURFACE LOAD

F = 800N

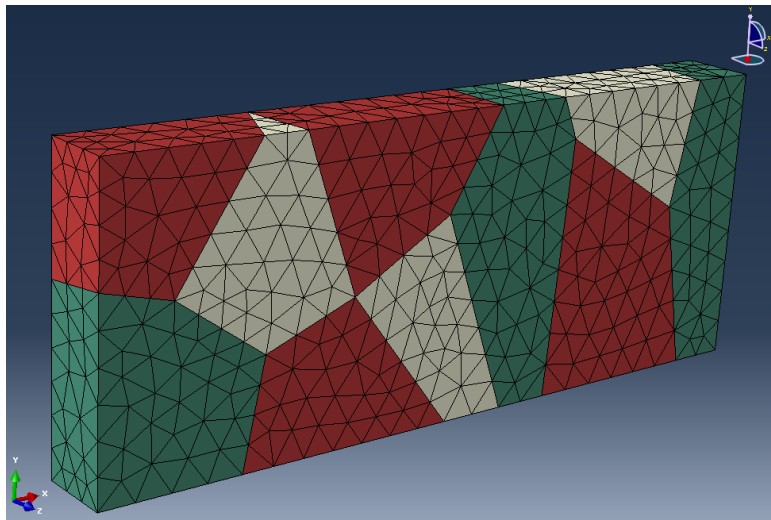
3-D POLYCRYSTALLINE MICROSTRUCTURE

Number of node: 1060
Number of element: 3939

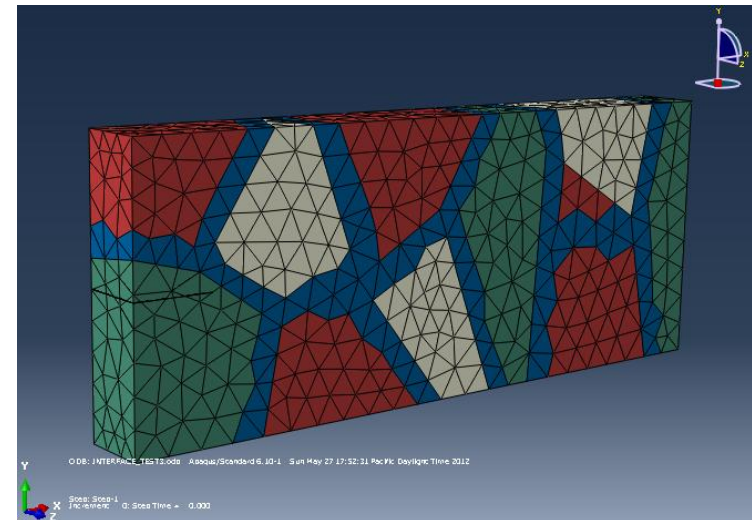


Initial crack of 20 microns are implemented to the model and each grain is assigned by one of three different material types.

To investigate the effect of grain boundary (GB), we conducted simulations: (1) without GB, (2) with GB

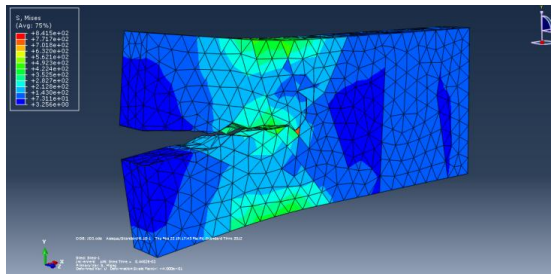
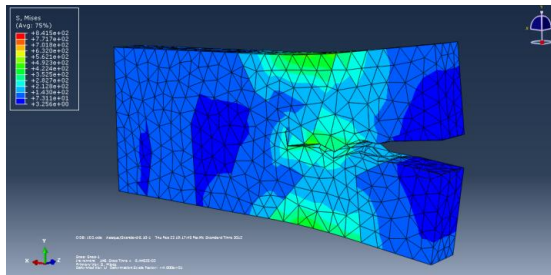
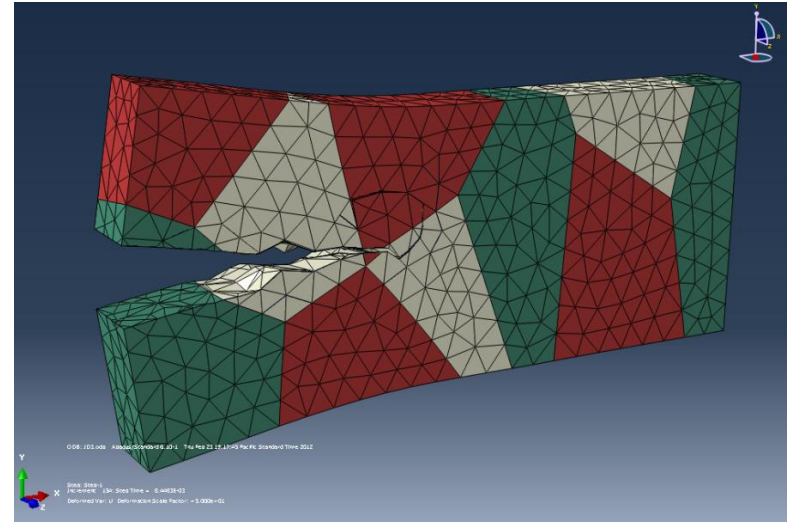
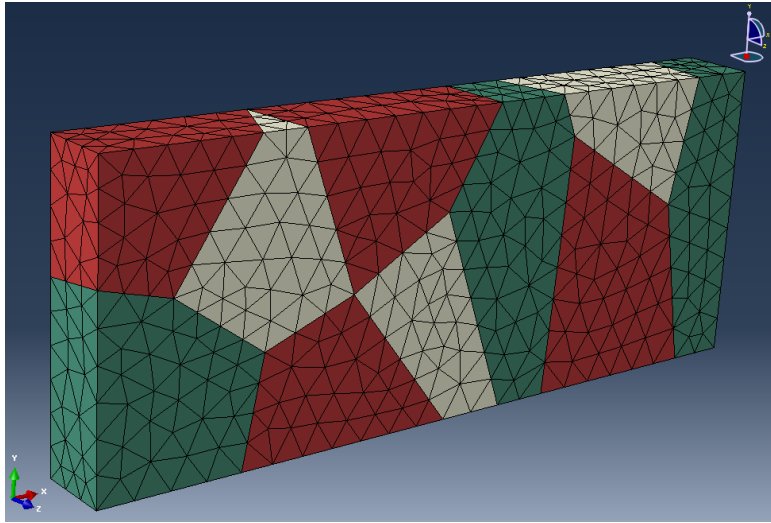


(1) without GB

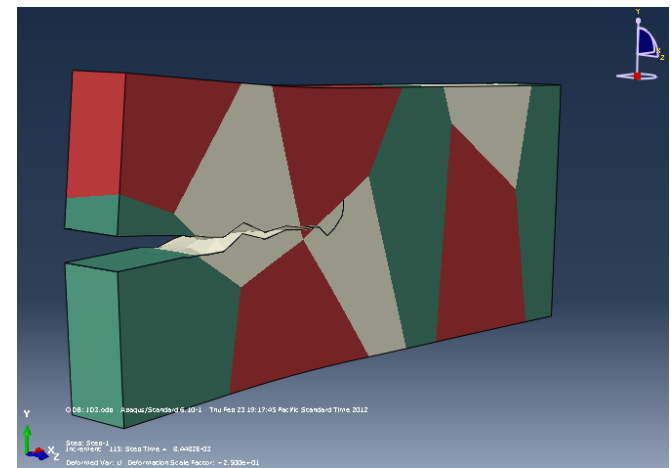


(2) with GB

SIMULATION WITHOUT INTERFACE (GRAIN BOUNDARY)

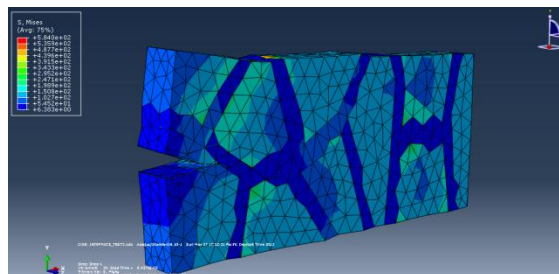
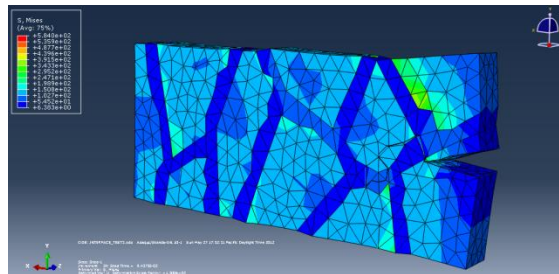
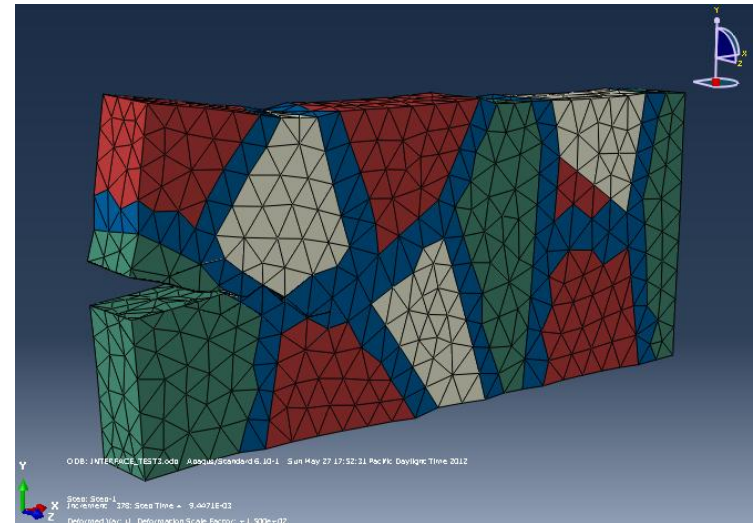
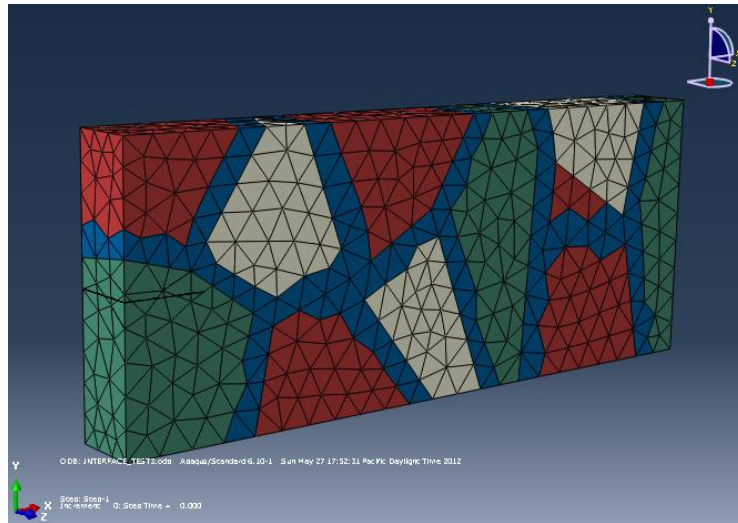


Mises stress contour

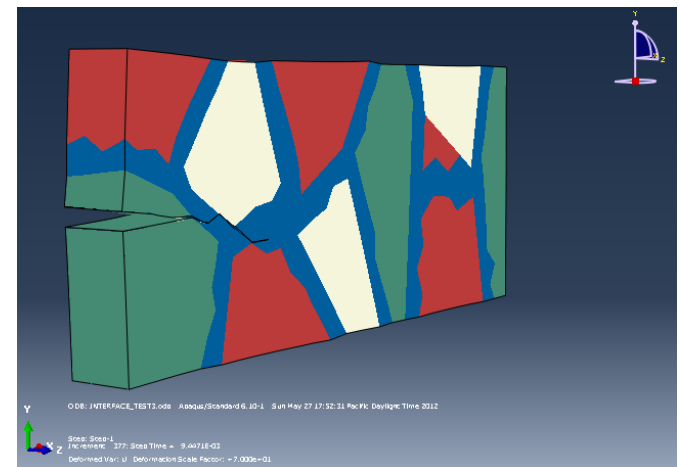


Mesh view disabled

SIMULATION WITHOUT INTERFACE (GRAIN BOUNDARY)



Mises stress contour



Mesh view disabled

Summary

In the CPMD calculation, we have

- Developed the atomic model of Ni-doped W for investigating the effect of amount of Ni addition to the material properties of tungsten.
- Conducted simulations with variation of temperature to find the relation of temperature to the material properties of tungsten.
- Obtained the stress-strain relations of each cases and developed the three-dimensional representation of relations.

In the XFEM simulation, we have

- Developed the model of three-dimensional polycrystalline microstructure of tungsten for prediction of crack pattern.
- Implemented GB parameters which were obtained from the CPMD calculation.
- Compared each cases for the crack patterns.

Future Work:

- More simulations with different polycrystalline models and validation.
- Develop a concept of XFEM and CFEM combined for improved prediction.
- Coupled Thermodynamics-Quantum-Multiscale Prediction of GB embrittlement